APPENDIX G

A COMPARISON OF SULFATE AND NITRATE PARTICLE MASS CONCENTRATIONS FROM IMPROVE AND THE CDN

G.1 INTRODUCTION

The Clean Air Status and Trends Network (CASTNet), or CASTNet Deposition Network (CDN) was established as a result of the 1990 Amendments to the Clean Air Act with the goal to determine the effect of emissions reductions mandated by the Act on air quality and deposition. Monitoring sites of the National Dry Deposition Network (NDDN), [CASTNet Report, 1998], itself established by the EPA in 1986, became a part of the CDN in 1992. Beginning in 1994, monitoring at 17 primarily western United States national parks began under the CDN, National Park Service (NPS), and EPA. The CDN monitoring program collects particle mass concentration data and meteorological parameters required to estimate dry particle deposition flux.

IMPROVE is primarily a visibility monitoring network, while the CDN was designed to estimate dry deposition. Each network has sampling protocols distinct from the other, although they both have a common interest in measurements of airborne species related to deposition and visibility related issues. If necessary data are available to initiate an inferential deposition model at IMPROVE sites, it would also be useful to use IMPROVE data to make estimates of dry particle deposition. Also, if necessary particle data, or estimates thereof, are available at CDN monitoring sites then one could use CDN data as a surrogate to estimate a visibility index (e.g., the particle light extinction coefficient) in regions where IMPROVE protocol data are not available. A first step is to see if concentrations from each respective network's sampling systems are comparable. We compare particle SO_4^{2-} and NO_3^- mass concentrations reported by the two networks using measurements from 23 locations where monitoring sites are within approximately 50 km.

Important differences between the samplers deployed by the CDN and IMPROVE networks should be kept in mind when comparing their respective data. For example, CDN protocol is to collect weekly integrated samples, while IMPROVE protocol is a twice a week 24-hour sampling schedule; CDN samplers are situated 10 m above ground level (agl), while IMPROVE sampler inlets are approximately 3 m agl; CDN samplers do not have size selective inlets, while IMPROVE samplers are fitted with either $PM_{2.5}$ or PM_{10} inlets; the CDN deploys filter pack samplers to measure all reported chemical components, while IMPROVE uses separate modules, including a denuded inlet (intended to remove HNO_3) for particle NO_3^- sampling. CDN collects particle nitrate on Teflon, while IMPROVE uses a nylon substrate to collect fine particle nitrate. Any of these protocol differences, as well as spatial variability introduced from geographical separation of selected comparison sites, could lead to an observed measurement bias.

Particle SO_4^{2-} is measured accurately by a variety of sampler configurations [Benner et al., 1991], while the magnitude of particle NO_3^- loss from Teflon is often significant [Shaw et al., 1982; Benner et al., 1991; Ashbaugh et al., 1998; Hering and Cass, 1999 and references therein]. Denuded samplers using nylon collection substrates have been found to provide more accurate particle NO_3^- measurements than filter pack methods that collect particle NO_3^- on Teflon [Shaw et al., 1982; Hering, 1986; Benner et al., 1991]. Direct comparisons of particle mass measured by IMPROVE samplers to measurements made by other similarly configured samplers (e.g., denuded samplers operating with cyclones) show good agreement between particle SO_4^{2-} and NH_4^{2+} mass concentrations, although agreement among particle NO_3^- measurements can be poor [Chow et al., 1994; Turpin et al., 1997].

The mass of particle NO_3^- measured by filter pack samplers can underestimate ambient particle NO_3^- mass under certain conditions. Ammonium nitrate can be lost on the filter by volatilization or by reaction with strong acid under ammonia limited conditions [Appel et al., 1984]. Field studies have shown the magnitude of NO_3^- loss from Teflon due to volatilization is temperature dependent [Hering and Cass, 1999]. Particle NO_3^- volatilization is dependent on the ammonium nitrate equilibrium constant, K, which has a strong dependence on temperature and humidity [Mozurkewich, 1993]. Alternatively, it is possible particle NO_3^- measured by a denuded Nylasorb substrate, such as used for particle NO_3^- sampling under IMPROVE protocol, will be overestimated if gas phase NO_3^- is not efficiently removed from the sample stream and consequently interpreted as particle NO_3^-.

Sampler inlet particle size cut points can also affect particle mass measurements depending on partitioning of ambient particles between fine (particles < approximately 2.5 μm in aerodynamic diameter) and coarse (particles > approximately 2.5 μm in aerodynamic diameter) size modes. Field studies indicate particle SO_4^{2-} resides predominantly in the fine mode in air masses of continental origin, while coarse particle NO_3^- may be present in both maritime and continental regimes [Harrison and Pio, 1983; Wolff, 1984; Wall et al., 1988].

If one accounts for the particle NO_3^- volatilization artifact alone, they might anticipate the CDN filter pack sampler to measure less particle NO_3^- mass than the denuded IMPROVE sampler. However, this anticipated bias relies on several assumptions: 1) particle NO_3^- measured by both networks exists as fine particles, 2) no measurement biases result from elevation or siting differences, and 3) IMPROVE denuders efficiently remove ambient HNO_3 without disturbing the ambient equilibrium partitioning of particle ammonium nitrate during sampling.

We attempt to reconcile the different sampling frequencies of the two monitoring networks by averaging, and address the question of how many consecutive IMPROVE sample periods must be averaged to form a reliable estimator of the population mean for a specified time period. The CDN data provide a useful benchmark for this analysis because those data ideally are continuous seven-day duration samples and should represent the population mean for a given sampling period. Averaging, of course, will not resolve bias due to spatial variability between comparison sites or non-random variability in the daily ambient mass concentrations. For example, if a monitoring site experiences a weekend pulse in particle mass concentration, the Wednesday Saturday sampling schedule may bias IMPROVE means over CDN means by preferential weighting of the weekend sample by IMPROVE.

We attempt to determine the magnitude, and multiplicative or additive nature, of observed biases between particle SO_4^{2-} and NO_3^- mass concentrations measured by the CDN and IMPROVE samplers. This analysis takes advantage of long-term monitoring data (up to ten years at some locations) that span all seasons and all observed meteorological conditions. Long-term data sets allow us to evaluate bias with greater statistical significance and to look for relationships between observed bias and external variables, such as aerosol composition and geographic region. Due to the many possible sources of bias between particle mass concentrations reported by the CDN and IMPROVE, including possible siting differences between respective comparison monitoring sites, this examination of the data does not constitute a controlled comparison study. Any inferred relationship to external factors is intended only as a clue to guide further investigations that may elucidate the mechanisms behind observed bias.

G.2 THE DATA

Detailed descriptions of the IMPROVE samplers are included in Chapter 1 and in related articles [Eldred et al., 1993; Malm et al., 1994]. For comparison to CDN data, IMPROVE particle mass concentrations are corrected to standard temperature of 25°C and standard pressure of 1013 mb using daily averaged temperature from meteorological measurements at IMPROVE sites. If the IMPROVE sites do not have an adequate temperature record for the comparison period, then these data are taken from CDN temperature measurements at the CDN comparison site.

Ambient particle and some gas phase measurements reported by the CDN are one-week integrated samples that begin on Tuesday and continue through the following Tuesday. The weekly samples are made using filter packs situated on a pole 10 m above ground. The CDN filter packs have a non-size selective inlet followed by three filters in series. The first filter is Teflon and is intended to collect particles, the second filter is nylon (Nylasorb) designed to collect ambient HNO_3, and the third is a dual K_2CO_3 impregnated cellulose filter designed to collect SO_2. All filters are extracted and analyzed by ion chromatography to determine the mass concentrations of collected ionic constituents. The CDN sampler flow rates are 1.50 l/min in the eastern United States and 3.00 l/min at sites in the western United States. The CDN data are reported at the same reference temperature and pressure used to correct IMPROVE data. Required meteorological, groundcover, and observational data are collected at each site to parameterize the Big Leaf deposition model [CASTNet Summary Report, 1998].

G.3 COMPARISON SITES

To compare particle mass concentrations from CDN and IMPROVE we use data from 23 monitoring site pairs that are separated by less than approximately 50 km and have suitable comparison data spanning approximately one year. The CDN and IMPROVE site names, horizontal separation in kilometers and vertical separation in meters, are listed in Table G.1. In Table G.1 the monitoring sites are separated into west, interior desert/mountain, and east regions of the United States. Figure G.1 is a map of the comparison sites labeled by their respective network site acronym.

Table G.1 *Horizontal and vertical distances between selected comparison sites from the CDN and IMPROVE network. Sites are shown sorted by geographic region. Elevation difference is the IMPROVE site elevation subtracted from the CDN site elevation.*

CDN Acronym	CDN Site Name	IMPROVE Acronym	IMPROVE Site Name	Δ Horizontal (km)	Δ Elevation (m)
West					
JOT	Joshua Tree NM	SAGO	San Gorgonio WA	80	-468
LAV	Lassen Volcanic NP	LAVO	Lassen Volcanic NP	41	-42
MOR	Mount Rainier NP	MORA	Mount Rainier NP	33	-1225
PIN	Pinnacles NM	PINN	Pinnacles NM	56	18
SEK	Sequoia NP	SEQU	Sequoia NP	52	676
YOS	Yosemite NP	YOSE	Yosemite NP	42	-10
Interior Desert/Mountain					
BBE	Big Bend NP	BIBE	Big Bend NP	1.5	-15
CAN	Canyonlands NP	CANY	Canyonlands NP	0.9	16
CHA	Chiricahua NM	CHIR	Chiricahua NM	16	-76
CNT	Centennial	BRLA	Brooklyn Lake	13	31
DEV	Death Valley NP	DEVA	Death Valley NP	2.0	3
GLR	Glacier NP	GLAC	Glacier NP	1.1	-396
GRB	Great Basin NP	GRBA	Great Basin NP	1.0	-13
GRC	Grand Canyon NP	GRCA	Grand Canyon NP	1.5	0
GTH	Gothic	WHRI	White River NF	25	-491
MEV	Mesa Verde NP	MEVE	Mesa Verde NP	0.9	-30
PND	Pinedale	BRID	Bridger WA	28	561
ROM	Rocky Mountain NP	ROMO	Rocky Mountain NP	3.1	20
YEL	Yellowstone NP	YELL	Yellowstone NP	39	549
East					
BEL	Beltsville	WASH	Washington, D.C.	55	43
LYE	Lye Brook	LYBR	Lye Brook	14	-261
PAR	Parsons	DOSO	Dolly Sods WA	20	-648
SHN	Shenandoah NP	SHEN	Shenandoah NP	8.6	-24

NP = National Park
NM = National Monument
WA = Wilderness Area
NF = National Forest

We recognize that the selected comparison sites are not collocated, and vertical as well as horizontal separation between some site pairs may introduce spatial bias. However, most of the selected monitoring sites are in remote areas where the mean particle SO_4^{2-} and NO_3^- mass concentrations are likely to be nearly uniform over areas larger than the distances that separate the respective comparison sites. Of course, the assumption of spatial homogeneity in mean ambient particle concentrations loses validity as the distance between monitoring site pairs increases and as the gradients in ambient particle concentration become steeper. For example, the majority of site pairs are within 100 m elevation, although respective monitoring sites

(MORA-MOR) have an elevation difference in excess of 1000 m. Elevation differences between sites can lead to diurnal and seasonal variability in measured particle mass. Similarly, the majority of site pairs are within 50 km, although the IMPROVE site at SAGO is approximately 80 km west of the CDN site at JOT. The distances between comparison sites are important to keep in mind when looking at results from this comparison analysis. Spatial bias cannot be separated from measurement bias related to particle sampler configuration by methods employed in this study.

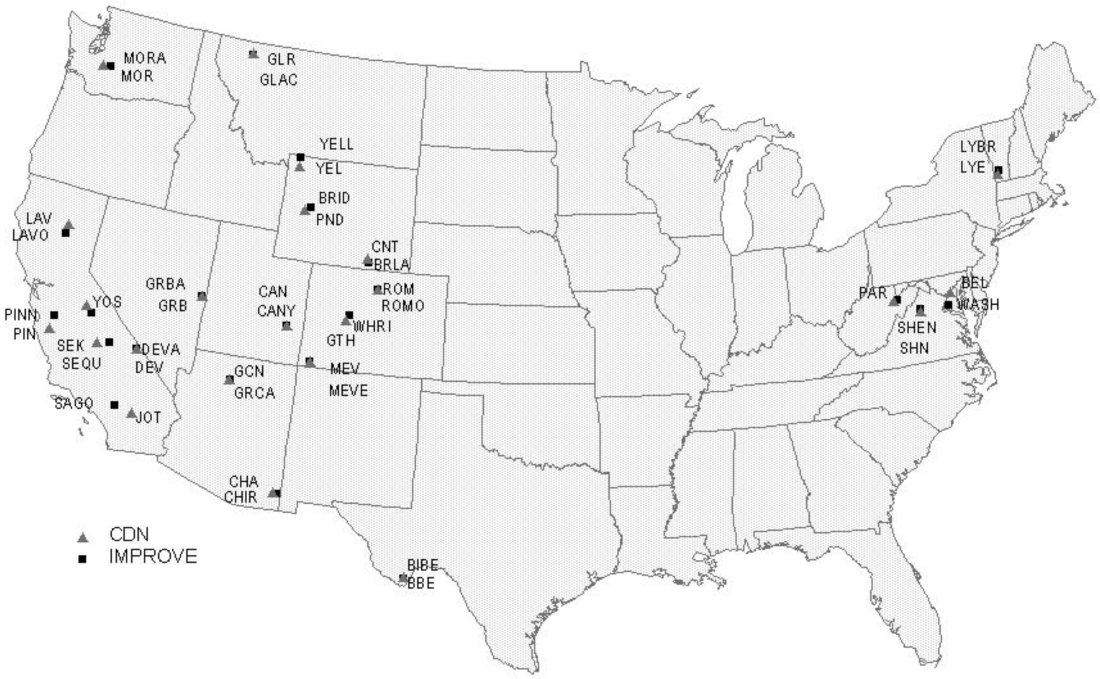

Figure G.1. *A map of comparison sites labeled by their respective network site acronym.*

G.4 RESULTS AND DISCUSSION

G.4.1 Averaging

We are interested in finding an optimal averaging time interval for IMPROVE data that is short enough to retain information about temporal variability in species mass concentrations, although long enough so that means from IMPROVE and the CDN would be indistinguishable, at a given confidence level, in the absence of a measurement bias for paired sites. This is relevant to a comparison of the respective network data because the networks sample with different frequencies. The IMPROVE protocol schedule introduces uncertainty in mean particle mass concentrations because only a fraction of the total days are sampled. This section examines the uncertainty in IMPROVE and CDN mean particle SO_4^{2-} and NO_3^- mass concentrations as a function of averaging time.

Paired CDN and IMPROVE data were selected for subsequent analysis using the criteria that CDN weekly samples had a duration of six to eight days and both 24-hour duration IMPROVE samples per week were present. IMPROVE data were averaged beginning with the first Wednesday sample and continuing through the final Saturday sample in any given averaging time interval, so that the IMPROVE samples coincide in time to the CDN Tuesday through Tuesday samples. Thus, the highest time resolution for data pairs is weekly data. Data pairs used in this section have a duration from one to 52 weeks.

One approach to estimate the uncertainty associated with the respective network means, or data pairs, is adapted from Iyer et al. [1999]. Sampling variance, in the context of sampling a fraction of the entire population, as is done under IMPROVE protocol, can be estimated by,

$$sv = \frac{s^2}{n}\left(1 - n/N\right) \tag{G.1}$$

where *sv* is the estimated sampling variance associated with less than continuous sampling frequency, and *s* is the standard deviation of *n* measurements out of *N* possible measurements. In Equation (G.1), *s* is an estimate of the population standard deviation on the time scale of *n*, and is assumed to represent random variability. An estimate of measurement standard error (*se*) at a given averaging time interval is calculated from the combined sampling and analytical variance,

$$se = \sqrt{sv + av} \tag{G.2}$$

where *av* is the analytical variance. We estimate *av* using a polynomial fit to reported IMPROVE measurement precision (σ), as a function of the respective chemical species mass concentration. For consistency, we apply the polynomial to both CDN and IMPROVE mass concentration data,

$$\sigma_{SO_4} = 0.0349 + 50.2580\left[SO_4^{2-}\right]^{-1.3052} \tag{G.3}$$

$$\sigma_{NO_3} = 0.0484 + 26.9609\left[NO_3^{-}\right]^{-1.3244} \tag{G.4}$$

where $[SO_4^{2-}]$ and $[NO_3^-]$ are particle mass concentrations in ng/m^3, and the species measurement precision is expressed as a fraction of the respective chemical species mass concentration. Equations (G.3) and (G.4) asymptote to measurement precisions of approximately 4% of SO_4^{2-}, and 5% of NO_3^- mass concentrations in excess of 1 μg/m^3. The *av* of *n* measurements is calculated from the individual species measurement precision, σ_i, by:

$$av = \sum_{i=1}^{n} \sigma_i^2 \Big/ n^2 \tag{G.5}$$

Similarly, we calculate the square of the mean *se* associated with more than one data pair (i.e., the mean *se* associated with 52 means calculated at 1-week averaging intervals) by summing the squares of the individual *se's* from Equation (G.2).

The approach outlined in Equations (G.1) to (G.5) has the advantage of estimating *se* without knowledge of a population mean or standard deviation. However, it has the disadvantage in that *sv* (from Equation (G.1)) is calculated using an estimate of the population standard deviation. Another approach to estimate IMPROVE *sv* at a given averaging time interval is to use departures of IMPROVE means from the population, or true, mean averaged over the same time interval. This approach requires knowledge of the population mean one seeks to represent by IMPROVE measurements.

We anticipate that means derived from the CDN data are essentially free of *sv* (in the absence of missing data). Therefore, we can then use means from the CDN to estimate the IMPROVE population mean, giving us another approach to estimate IMPROVE measurement uncertainty. To do so, we form data pairs from the respective networks at averaging time intervals ranging from one to 52-weeks. We denote the difference between individual data pairs as $d_{1..n}$, where n is the number of pairs, and we use D to denote the mean of $d_{1..n}$. This approach allows us to exclude much of the variability common to both networks, and thereby estimate the magnitude of *se* in IMPROVE means arising primarily from the IMPROVE sampling frequency, as a function of averaging time interval. The IMPROVE *se* in the difference approach is assumed to be represented by the standard deviation of $d_{1..n}$. Another assumption in this approach is that the respective network samplers are measuring the same quantity. That is, the respective network measurements are free of bias introduced by spatial and/or temporal variability between samplers.

Figure G.2 compares results from the two approaches. Figure G.2 shows the mean *se* associated with particle SO_4^{2-} mass concentrations from the CDN (diamonds) and IMPROVE (triangles), as calculated in Equations (G.1) to (G.5), and *se* associated with the difference (squares). Averaging time intervals shown in Figure G.2 range from one to 52-weeks and the mean *se's* shown incorporate the same number of samples regardless of averaging interval. We show data for five long-term sites, all of which have approximately 10 years of comparison data, so that the data include all seasons and ranges of expected particle mass concentrations.

Figure G.2 indicates the *se* associated with the CDN means is essentially constant as a function of averaging time interval. This is expected because the CDN data are continuous and *se* is determined by *av*, the mean of which is essentially constant for long-term data. The *se* associated with the IMPROVE means combines *sv* and *av*, and decreases with increasing averaging because *sv* (in Equation (G.1)) decreases as the number of samples incorporated in the averaging interval increases. Similarly, the IMPROVE *se* estimated from D decreases with increasing averaging time interval. Figure G.2 shows that for SO_4^{2-}, the *se* estimated from D is generally equivalent to or less than the IMPROVE *se* (from Equation (G.5)) at the same averaging time interval. It appears that at averaging time intervals of 1-week the IMPROVE *se* may be underestimated by using Equations (G.1) to (G.5). At longer averaging time intervals, the IMPROVE *se* may be overestimated by Equations (G.1) to (G.5) due to the incorporation of long-term variability of particle SO_4^{2-} mass concentration in the estimated population s in Equation (G.1). Long-term variability arises from the strong seasonal cycle in particle SO_4^{2-} mass concentrations, which is common to both networks and should not be included in the uncertainty estimates of IMPROVE means. This common variability is removed by estimating IMPROVE *se* by difference method. Based on the SO_4^{2-} data it appears that the difference approach gives a reasonable approximation of the uncertainty in means of IMPROVE measurements.

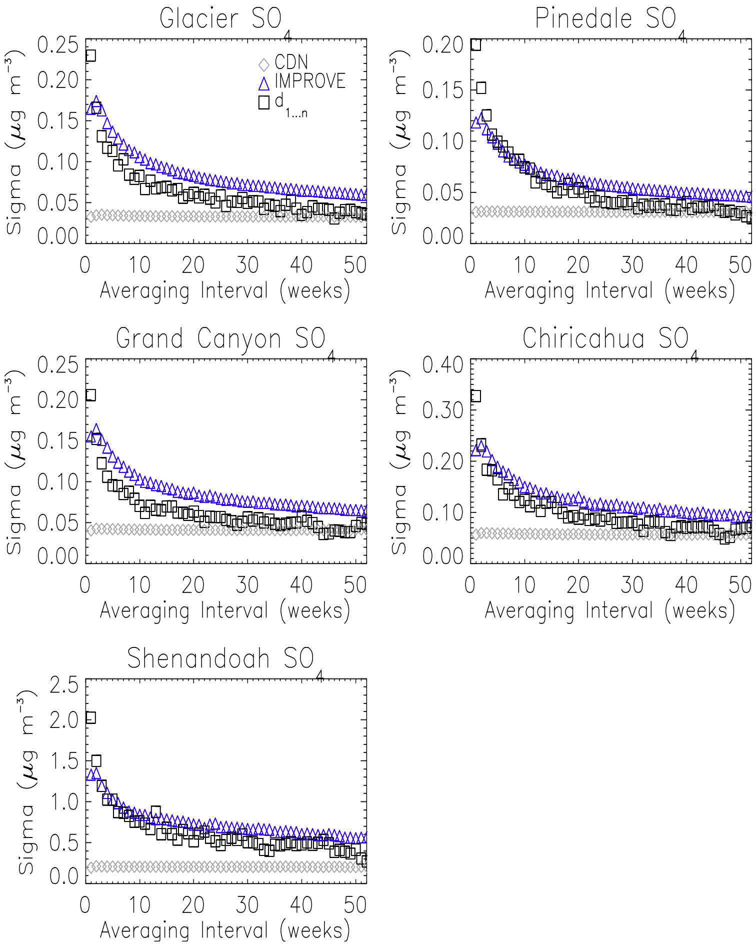

Figure G.2. *Particle SO_4^{2-} mass concentration se (sigma) for IMPROVE (triangles), CDN (diamonds) and the se for the difference between paired measurements, $d_{1..n}$ (squares), shown as a function of averaging time interval.*

Figure G.3 is analogous to Figure G.2, but shows the *se* associated with mean particle NO_3^- mass concentrations as a function of averaging time interval. From Figure G.3 we see that the *se* associated with CDN mean is again determined by *av*, and furthermore, that the *se* associated with the IMPROVE mean decreases with increasing averaging time interval. The main discrepancy between uncertainty estimates shown in Figures G.2 and G.3 is the relatively poor agreement between the two approaches used to estimate the *se* in IMPROVE mean. In almost all cases in Figure G.3 the IMPROVE *se* calculated using Equations (G.1) to (G.5) is less than the *se* estimated by the difference approach. This poor agreement could be explained by the fact that the CDN and IMPROVE samplers are not measuring the same quantity, suggesting a particle NO_3^- measurement bias between the two networks.

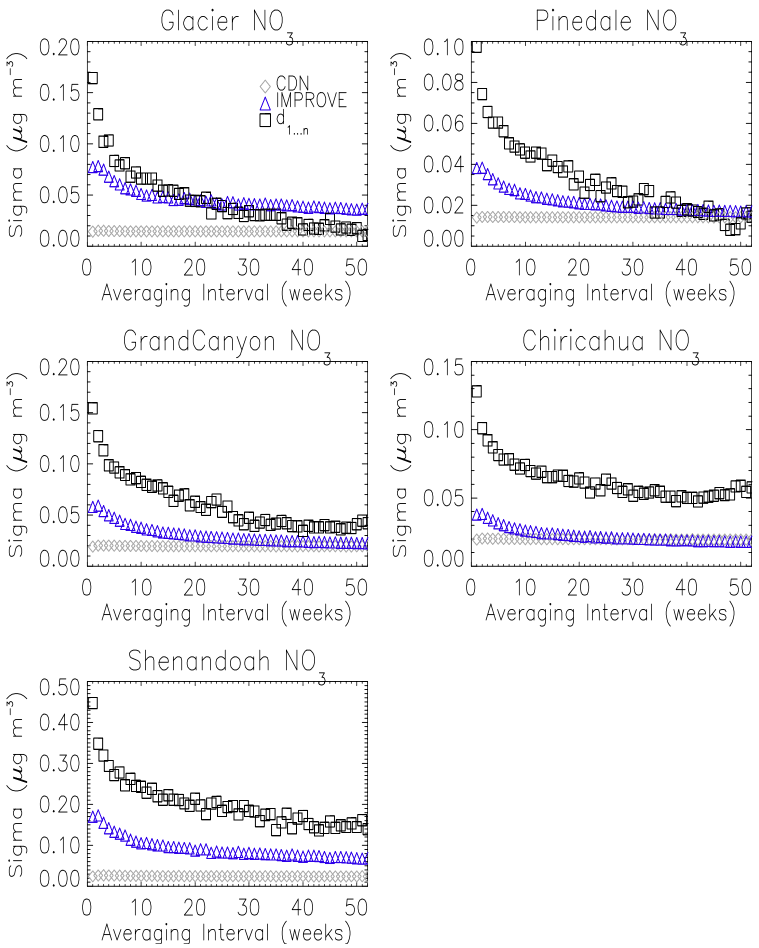

Figure G.3. *Particle NO_3^- mass concentration se (sigma) for IMPROVE (triangles), CDN (diamonds) and the se for the difference between paired measurements, $d_{1..n}$ (squares), shown as a function of averaging time interval..*

The *se* associated with the IMPROVE and CDN means is an estimate of the magnitude of uncertainty in the respective means at a given averaging time interval, where one *se* corresponds to an 84% confidence interval, based on a normal distribution. Values of the IMPROVE *se*, expressed as a percent of the mean IMPROVE particle SO_4^{2-} mass concentration, are shown in Table G.2 for selected averaging time intervals. Table G.2 compares values from the approach using Equations (G.1) to (G.5), denoted as *se(sv)*, and the approach using the *se* of *D*, denoted as *se(D)*. For SO_4^{2-}, the two approaches give similar results, with *se(D)* slightly lower than *se(sv)* at all but 1- to 2-week averaging intervals. Among the sites shown in Table G.2 the IMPROVE SO_4^{2-} *se* at a 1-week averaging time interval is as high as 30% and at 52 weeks the *se* is as low as 4%.

Values of the IMPROVE particle NO_3^- *se*, expressed as a percent of the mean IMPROVE mass concentration, are also shown in Table G.2. For particle NO_3^-, the two approaches do not compare well, with *se(D)* generally higher than *se(sv)*, reflecting results shown in Figure G.3. Table G.2 shows that at 1-week averaging time intervals the IMPROVE particle NO_3^- *se(sv)* is as high as 30% and *se(D)* is as high as 90%. At 52-week averaging intervals, the *se* is as low as 4%. For reasons mentioned earlier, *se(D)* may not be a reasonable approximation of uncertainty associated with the IMPROVE mean. Also, *se(sv)* may underestimate IMPROVE measurement uncertainty at 1-week averaging intervals.

Table G.2. *Standard error (se) in IMPROVE particle SO_4^{2-} and NO_3^- mass concentration measurements as a function of averaging time interval at five long-term monitoring locations. The se is expressed as a percent of the respective IMPROVE chemical species mean particle mass concentration, and represents the mean se at the specified averaging interval for all available data at each site. Two methods are used to calculate se, se(sv) refers to the se obtained from Equations (G.1) to (G.5) in the text, while se(D) refers to the se associated with the difference between paired IMPROVE and CDN.*

Site	**Averaging Interval (weeks)**	**SO_4^{2-} *se(sv)* (%)**	**SO_4^{2-} *se(D)* (%)**	**NO_3^- *se(sv)* (%)**	**NO_3^- *se(D)* (%)**
Glacier	1	21	29	31	65
	2	22	21	31	51
	4	19	15	27	41
	13	12	8	19	23
	26	9	6	17	13
	52	7	4	14	4
Pinedale	1	19	31	30	76
	2	20	25	30	58
	4	17	17	26	47
	13	11	10	19	35
	26	9	6	15	24
	52	7	4	13	11
Grand Canyon	1	16	22	31	81
	2	17	16	31	67
	4	15	11	26	52
	13	10	7	18	41
	26	8	6	15	31
	52	7	5	12	22
Chiricahua	1	16	23	25	86
	2	16	17	26	68
	4	14	13	23	58
	13	10	7	16	46
	26	8	6	14	40
	52	7	5	12	38
Shenandoah	1	24	37	27	72
	2	24	27	28	56
	4	20	18	23	47
	13	14	16	16	35
	26	12	9	13	30
	52	10	5	10	21

Based on this analysis, we recommend using at least four weeks of IMPROVE particle SO_4^{2-} measurements to form a reliable estimate of the population mean. Variability in measured particle NO_3^-, relative to observed mean mass concentration, is greater than for particle SO_4^{2-}, and therefore we recommend that approximately 13-weeks of data from IMPROVE to estimate a population mean for particle NO_3^-. These suggested averaging time intervals correspond to the averaging required to reduce the uncertainty in the IMPROVE chemical species mean particle mass concentration to approximately 10 to 20%. Note that the analysis in this section is intended to estimate mean uncertainties in IMPROVE and CDN particle mass concentrations at specified averaging times, and is not necessarily intended to demonstrate uncertainties associated with long-term means. The latter is addressed in the following section using other statistical methods.

G.4.2 Regression Analysis and Comparison of Means

For the regression analysis and comparison of means, data from each network are paired and averaged to produce 4-week means, as described in the previous section. Averaging reduces sampling variance related to the twice a week IMPROVE sampling frequency, and is intended to give the comparison more physical significance related to differences between the respective network's sampler configurations. We explicitly look for multiplicative bias using the nonparametric Theil approach [Theil, 1950] and using a modified Theil approach to derive the slope intercept as an estimate of additive bias [Graybill and Iyer, 1994]. We chose a nonparametric regression because it is unbiased to extreme and outlying values. To determine the confidence level at which the difference in mean particle SO_4^{2-} and NO_3^- mass concentrations measured by the respective networks is significant we use a paired T-test, which is appropriate for data expected to have serial correlation.

G.4.2.1 Sulfate

Figure G.4 shows scatter plots of particle SO_4^{2-} mass concentrations data pairs from the CDN and IMPROVE at all 23 comparison sites, labeled by the CDN site name. Also shown in Figure G.4 are the 1:1 line and error bars representing one standard error (*se*) in the data pairs from each network. The *se* shown is calculated from Equation (G.2). Figure G.4 shows that the magnitude of *se* in the IMPROVE 4-week means is generally larger than in the CDN means, due to the contribution of sampling variance from IMPROVE sampling frequency, as discussed earlier. The mean *se* in 4-week averaged particle SO_4^{2-} mass concentrations shown in Figure G.4 is ±5% of the respective CDN means and ±19% of the IMPROVE means. Table G.3 lists the respective site pair acronyms (refer to Table G.1 for site names) and comparison statistics. Included in Table G.3 are the paired IMPROVE and CDN particle SO_4^{2-} mass concentration Theil regression intercepts (b_o) and slopes (b_1), with respective P-values. The P-value associated with b_o gives the lowest level at which we can reject the hypothesis that b_o is zero. The P-value associated with the regression slope gives the lowest level at which we can reject the hypothesis that b_1 is one. That is, if b_o P is less than 0.05 we can be 95% confident that the intercept is not equal to zero. N is the number of data pairs used in the regressions and to calculate means (X is CDN, Y is IMPROVE) shown in Table G.3. Means of X and Y and the P-value associated with the paired T-test are also shown in Table G.3, with start and stop dates corresponding to the initial and final month/year of the weekly comparison data, respectively.

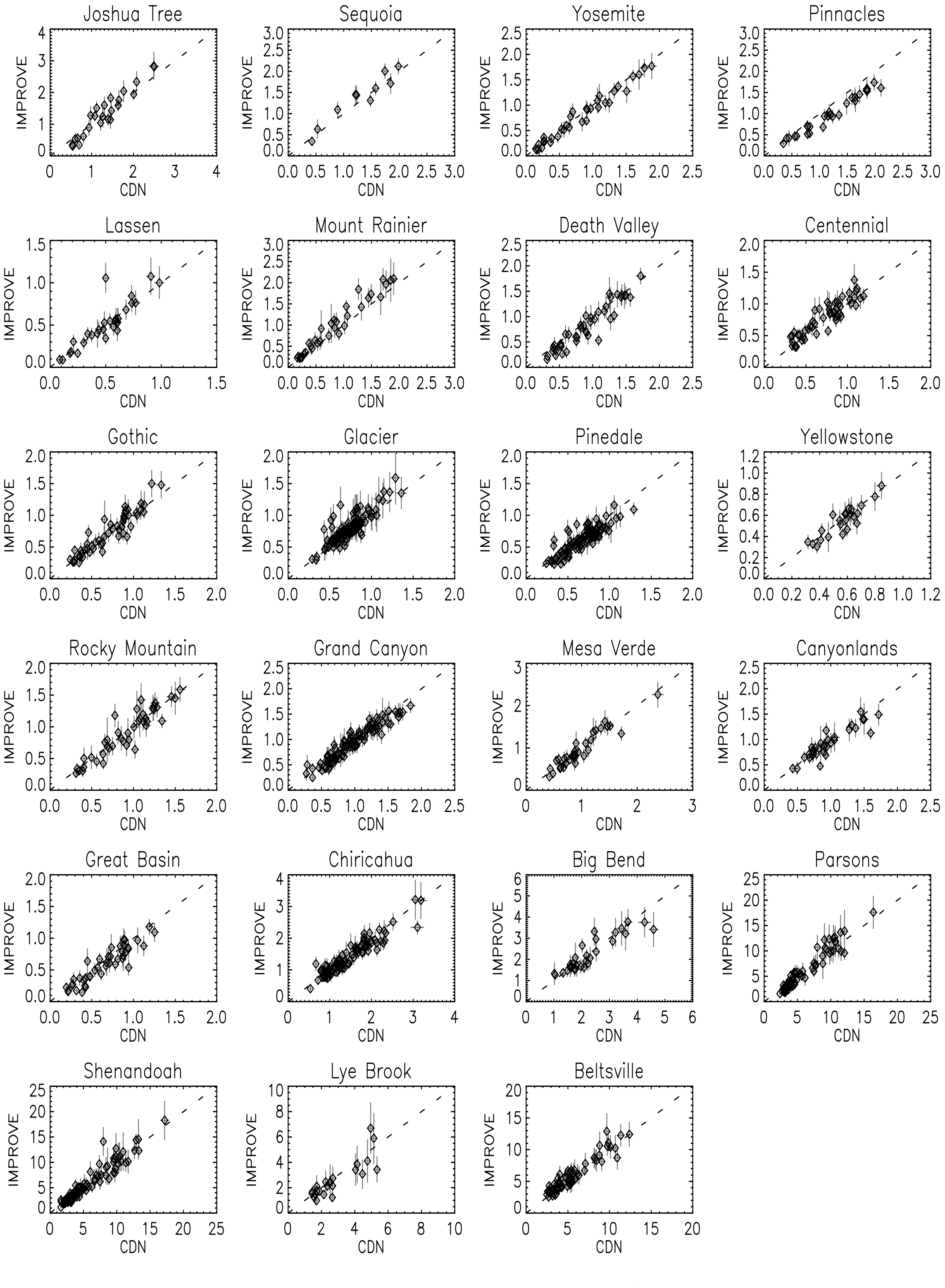

Figure G.4 *Comparison of IMPROVE and CDN particle SO_4^{2-} mass concentrations ($\mu g/m^3$) at 23 comparison sites. Scatter plots show 4-week means and error bars indicate ± one standard error in the respective network means.*

For the particle SO_4^{2-} comparison, Theil regression slopes are close to one and intercepts close to zero. Regression slopes are significant at the 95% confidence level at nine comparison sites, indicating multiplicative bias, and the regression intercepts are significant at two sites, indicating additive bias. Site pairs with significant slopes range in magnitude from 0.81 at BBE to 1.22 at JOT (site pairs are referred to in the text by their CDN acronym, as given in Table G.1).

Table G.3 *Particle SO_4^{2-} regression results from 23 CDN and IMPROVE comparison sites, separated by geographic region. Site acronyms are shown for each monitoring network. Statistics are described in the text.*

SITE ACRONYM **CDN**	 **IMPROVE**	**b_0** **μg/m^3**	**b_0 P**	**b_1**	**b_1 P**	**N**	**X_{ave}** **μg/m^3**	**Y_{ave}** **μg/m^3**	**X-Y P**	**Start**	**Stop**
West											
JOT	SAGO	0.14	0.387	1.22	0.013	24	1.32	1.35	0.506	2/95	12/98
LAV	LAVO	-0.03	0.212	1.01	0.809	29	0.50	0.50	0.747	7/95	12/98
MOR	MORA	0.01	0.598	1.12	0.011	32	0.86	1.00	0.000	11/95	12/98
PIN	PINN	0.03	0.500	0.83	0.000	27	1.19	0.98	0.000	5/95	11/98
SEK	SEQU	0.04	0.500	1.02	0.727	10	1.29	1.37	0.156	2/97	12/98
YOS	YOSE	-0.01	0.500	0.95	0.060	34	0.82	0.78	0.010	10/95	12/98
Interior Desert/ Mountain											
BBE	BIBE	0.48	0.212	0.81	0.025	29	2.30	2.25	0.497	8/95	12/98
CAN	CANY	0.00	0.598	0.85	0.010	33	0.97	0.92	0.046	3/95	12/98
CHA	CHIR	0.07	0.386	0.91	0.023	96	1.46	1.40	0.003	5/89	11/98
CNT	BRLA	0.19	0.115	0.94	0.269	51	0.73	0.79	0.001	9/93	12/98
DEV	DEVA	-0.03	0.500	1.05	0.363	43	0.90	0.80	0.000	2/95	12/98
GLR	GLAC	0.24	0.022	0.97	0.522	111	0.73	0.79	0.000	4/89	12/98
GRB	GRBA	0.03	0.500	0.91	0.143	43	0.66	0.59	0.000	5/95	12/98
GRC	GRCA	-0.02	0.443	0.94	0.042	99	0.97	0.94	0.003	6/89	8/98
GTH	WHRI	-0.08	0.347	1.05	0.312	52	0.70	0.73	0.105	7/93	12/98
MEV	MEVE	0.34	0.105	1.04	0.642	33	0.98	0.97	0.561	1/95	11/98
PND	BRID	0.07	0.198	0.86	0.001	100	0.67	0.62	0.000	1/89	12/98
ROM	ROMO	0.19	0.095	1.04	0.481	42	0.91	0.90	0.757	1/95	12/98
YEL	YELL	-0.08	0.500	0.99	0.958	23	0.57	0.55	0.134	7/96	12/98
East											
BEL	WASH	-0.42	0.569	0.96	0.350	66	5.51	5.86	0.001	1/90	10/98
LYE	LYBR	0.19	0.500	0.82	0.248	23	2.86	2.61	0.126	5/94	11/98
PAR	DOSO	-1.23	0.001	1.15	0.004	77	5.79	5.72	0.535	9/91	11/98
SHN	SHEN	-0.12	0.286	1.03	0.520	100	5.47	5.57	0.307	1/89	12/98

Twelve site pairs indicate significant differences in mean particle SO_4^{2-} mass by paired T-test. The magnitude of significant difference (the IMPROVE mean subtracted from the CDN mean, expressed as a percent of the IMPROVE mean) ranges from 22% at PIN to –14% at MOR. The mean relative difference in SO_4^{2-} is 0% for each of the three regions shown in Table G.4, and the root mean square (RMS) relative difference among all 23 comparison sites is 8%. Bearing in mind that spatial variability may account for some observed bias, this result indicates surprisingly good comparability for the respective particle SO_4^{2-} measurements.

Comparison site pairs with significant differences in mean particle SO_4^{2-} mass concentrations are not necessarily the same comparison sites that show significance in one or both regression terms. A possible explanation is that the paired difference test removes variability common to both data sets, while regression analysis relies on a linear model to account for common variability, which may not be appropriate to explain differences in particle mass concentrations observed at all comparison sites during all seasons.

G.4.2.2 Nitrate

Figure G.5 shows scatter plots of paired particle NO_3^- mass concentration data for the CDN and IMPROVE at the 20 comparison sites with particle NO_3^- data, with the 1:1 line and error bars representing one *se* in the data pairs from each network, analogous to Figure G.4 for SO_4^{2-}. The mean *se* in 4-week averaged particle NO_3^- mass concentrations shown in Figure G.5 is ±7% for the CDN data and ±26% for the IMPROVE data. Table G.4 lists regression statistics and means for the CDN and IMPROVE particle NO_3^- mass concentration data, analogous to Table G.3 for SO_4^{2-}. We use 4-week NO_3^- means so that all sites have sufficient comparison data pairs for the regression and paired T-test. While this is a shorter time period than the 13-week averaging time recommended in Section G.4.1 to estimate the population mean at a given confidence level, the regression and paired T-test analysis in this section make use of a minimum of ten 4-week means.

Table G.4 shows the particle NO_3^- regression slope at six comparison sites is indistinguishable from one, while the remaining sites have slopes significantly less than one at the 95% confidence level. The magnitude of significant regression slopes ranges from 0.68 at LAV to 0.34 at BBE. A slope less than one indicates particle NO_3^- measured by the CDN is multiplicatively biased higher than the corresponding IMPROVE data. The particle NO_3^- regression intercepts at all comparison sites are either indistinguishable from or greater than zero at the same confidence level. The largest magnitude particle NO_3^- regression intercepts are at the BEL and JOT comparison sites.

The paired T-test indicates differences in mean particle NO_3^- mass are significant at the 95% confidence level at all but three comparison site pairs, with means from CDN predominantly greater than means from IMPROVE, or a positive CDN bias, in all geographic regions indicated in Table G.4, except in the East. The magnitude of relative difference in particle NO_3^- mass concentrations (the IMPROVE mean subtracted from the CDN mean (X_{ave}-Y_{ave}) from Table G.4), expressed as a percent of the IMPROVE mean, or $\Delta NO_3^-\%$) ranges from 151% at BBE to -29% at SHN. The minimum relative difference among non-eastern sites is –28% at GLR. The average $\Delta NO_3^-\%$ by region is 40% in the West, 56% in the interior desert/mountain region, and -9% in the East. The RMS mass concentrations difference, among 18 of 20 particle NO_3^- comparison sites, is 59%, when expressed as a percent of the IMPROVE means, or 35% when expressed as a percent of the CDN means.

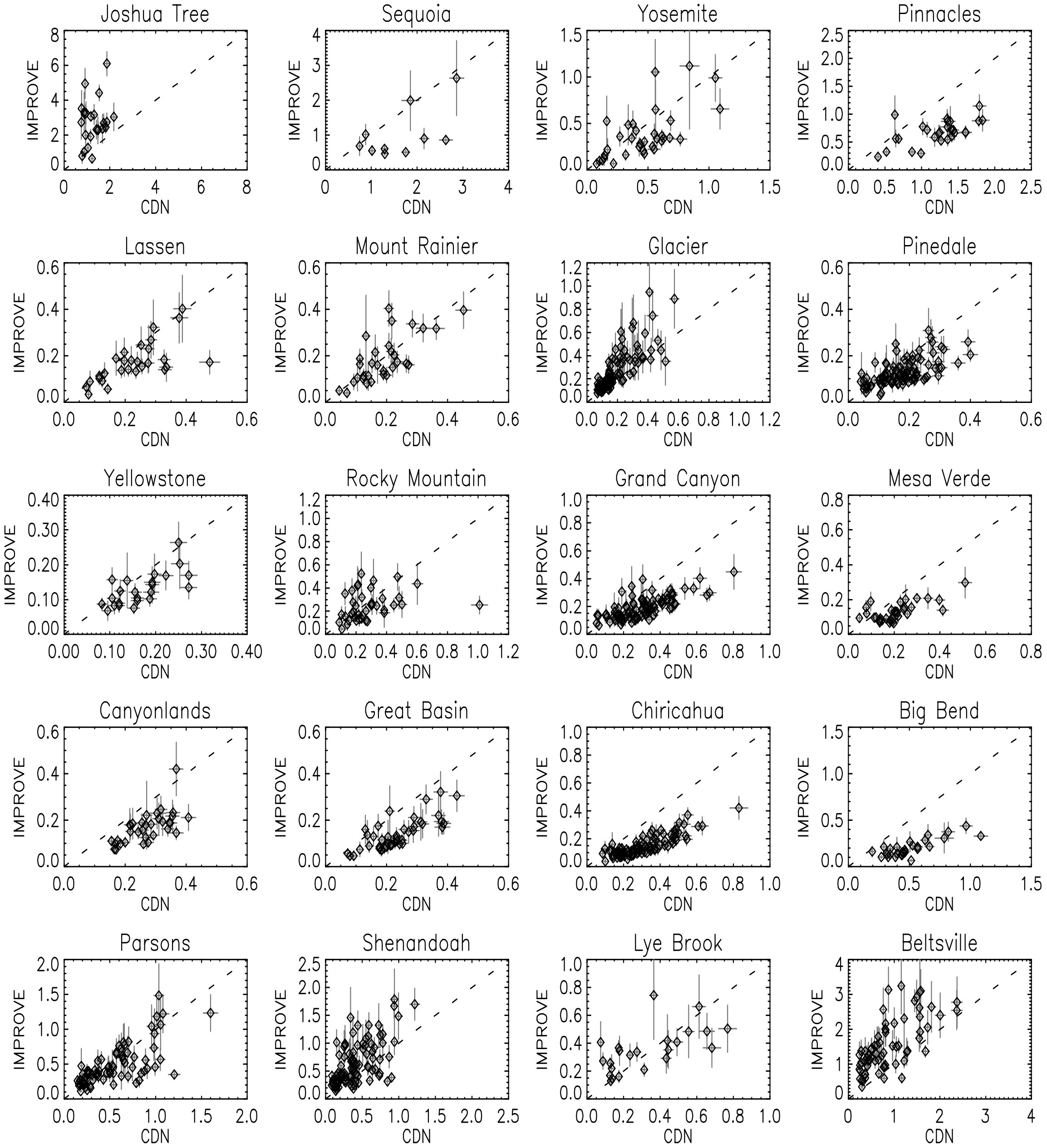

Figure G.5 *Comparison of IMPROVE and CDN particle NO_3^- mass concentrations ($\mu g/m^3$) at 20 comparison sites. Scatter plots show 4-week means and error bars indicate ± one standard error in the respective network means.*

Table G.4 *Particle NO_3^- regression results, mean mass concentrations, and comparison time periods for the 20 CDN and IMPROVE sites pairs, analogous to Table G.3. Site acronyms are shown for each monitoring network. Statistics are described in the text*

SITE ACRONYM		**b_0**	**b_0 P**	**b_1**	**b_1 P**	**N**	**X_{ave}**	**Y_{ave}**	**X-Y P**	**Start**	**Stop**
CDN	**IMPROVE**	**$\mu g/m^3$**					**$\mu g/m^3$**	**$\mu g/m^3$**			
West											
JOT	SAGO	2.21	0.073	0.67	0.476	24	1.28	2.73	0.000	2/95	12/98
LAV	LAVO	-0.01	0.605	0.68	0.025	28	0.23	0.17	0.001	7/95	11/98
MOR	MORA	0.00	0.500	0.78	0.114	31	0.19	0.19	0.728	11/95	11/98
PIN	PINN	0.10	0.133	0.37	0.000	27	1.22	0.67	0.000	5/95	11/98
SEK	SEQU	0.24	0.500	0.19	0.073	10	1.65	1.02	0.014	2/97	12/98
YOS	YOSE	0.06	0.072	0.53	0.002	34	0.46	0.37	0.020	10/95	12/98
Interior Desert/ Mountain											
BBE	BIBE	0.05	0.605	0.34	0.000	29	0.50	0.20	0.000	8/95	12/98
CAN	CANY	-0.07	0.105	0.56	0.001	33	0.27	0.17	0.000	3/95	12/98
CHA	CHIR	0.05	0.042	0.39	0.000	97	0.31	0.15	0.000	5/89	12/98
GLR	GLAC	0.06	0.091	1.11	0.165	112	0.18	0.25	0.000	2/89	11/98
GRB	GRBA	-0.02	0.500	0.54	0.000	43	0.23	0.14	0.000	5/95	12/98
GRC	GRCA	0.06	0.012	0.39	0.000	101	0.30	0.19	0.000	7/89	8/98
MEV	MEVE	0.04	0.105	0.37	0.000	33	0.21	0.13	0.000	1/95	11/98
PND	BRID	0.05	0.045	0.39	0.000	101	0.18	0.13	0.000	1/89	12/98
ROM	ROMO	0.26	0.058	0.40	0.000	41	0.28	0.25	0.203	1/95	12/98
YEL	YELL	0.01	0.500	0.57	0.006	23	0.17	0.13	0.000	7/96	12/98
East											
BEL	WASH	0.82	0.000	1.02	0.947	70	0.86	1.53	0.000	1/90	10/98
LYE	LYBR	0.23	0.113	0.43	0.000	23	0.33	0.35	0.583	5/94	11/98
PAR	DOSO	0.16	0.026	0.64	0.000	77	0.54	0.48	0.018	9/91	11/98
SHN	SHEN	0.21	0.000	0.96	0.716	102	0.41	0.63	0.000	1/89	12/98

Spatial variability in ambient particle NO_3^- between site pairs may cause some of the observed bias in particle NO_3^- measurements. For example, the IMPROVE site SAGO is about 50 km closer to the Los Angeles basin, and has a two-fold higher mean particle NO_3^- mass concentration than the CDN site JOT. Also, a large magnitude difference is observed between mean particle NO_3^- at the IMPROVE site WASH, which is in an urban setting, and the CDN site BEL, 20 km to the north. The observed differences between means at these site pairs may be related to spatial variability. Both site pairs have large magnitude regression intercepts, which may account for much of the observed bias between mean particle mass concentration. However, we do not imply that spatial variability will necessarily be manifest in the regression intercept. Based on their geographic separation alone, spatial variability may account for some of the observed bias at the JOT and BEL site pairs, and comparison data from these two sites are excluded from the summary in the preceding paragraph, and from any subsequent discussion.

A cursory examination of the data shows that the further south the sampling location, the larger the relative magnitude of particle NO_3^- bias. Figure G.6 is a plot of site latitude vs. relative particle NO_3^- mass concentration difference ($\Delta NO_3^-\%$) for 15 comparison sites in the West and interior desert/mountain regions, with the CDN site acronyms shown for each site pair. Figure G.6 demonstrates an increasing positive CDN particle NO_3^- bias with decreasing site latitude, suggesting factors related to site geography influence the observed bias. An analogous geographic trend is observed in the particle NO_3^- regression slope, although not in the regression intercept. Comparison sites in the eastern United States are not shown in Figure G.6 because the small number of comparison sites in this region make any geographic trends difficult to resolve.

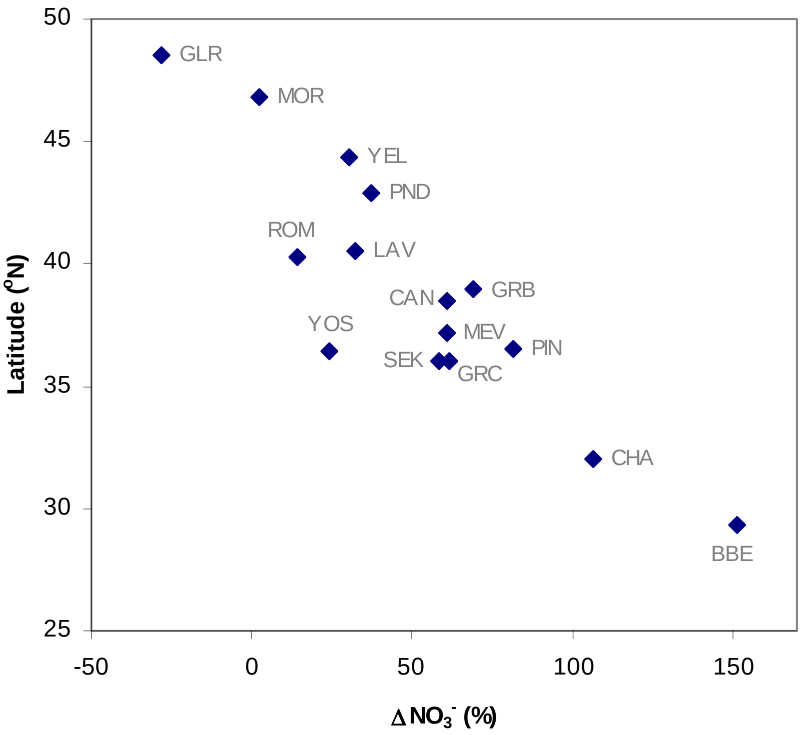

Figure G.6 *Site latitude vs. relative difference in mean particle NO_3^- mass concentration (expressed as the IMPROVE mean subtracted from the CDN mean as a percent of the IMPROVE mean) for 16 comparison sites in the western and interior desert/mountain regions.*

G.4.3 Comparison of Seasonal Means

G.4.3.1 Sulfate

Figure G.7a shows the absolute difference (IMPROVE subtracted from CDN as a percent of the IMPROVE mean) in mean particle SO_4^{2-} mass concentration for the winter (DJF), spring (MAM), summer (JJA), and autumn (SON) seasons. The IMPROVE site acronyms are shown to identify the respective site pairs. Figure G.7b shows the same difference expressed as a percent of the IMPROVE means. In Figure G.7a and G.7b, wintertime data at SEK-SEQU are not shown due to lack of sufficient comparison data during this season. Large differences in absolute SO_4^{2-} mass concentration are observed at comparison sites in the East, particularly during the summer when ambient SO_4^{2-} concentrations are high, however on a relative basis differences in the East are comparable to relative differences observed in other regions. Large relative differences in SO_4^{2-} mass concentrations (on the order of 20% or more) are observed at a number of comparison sites. Frequently, the relative differences are greatest during the winter, when low level inversions are likely to cause spatial sampling variability between sites with large vertical separation. For example, the IMPROVE site at DOSO is 648 m higher than the CDN site at PAR, which could explain higher particle mass concentrations at the lower elevation CDN site.

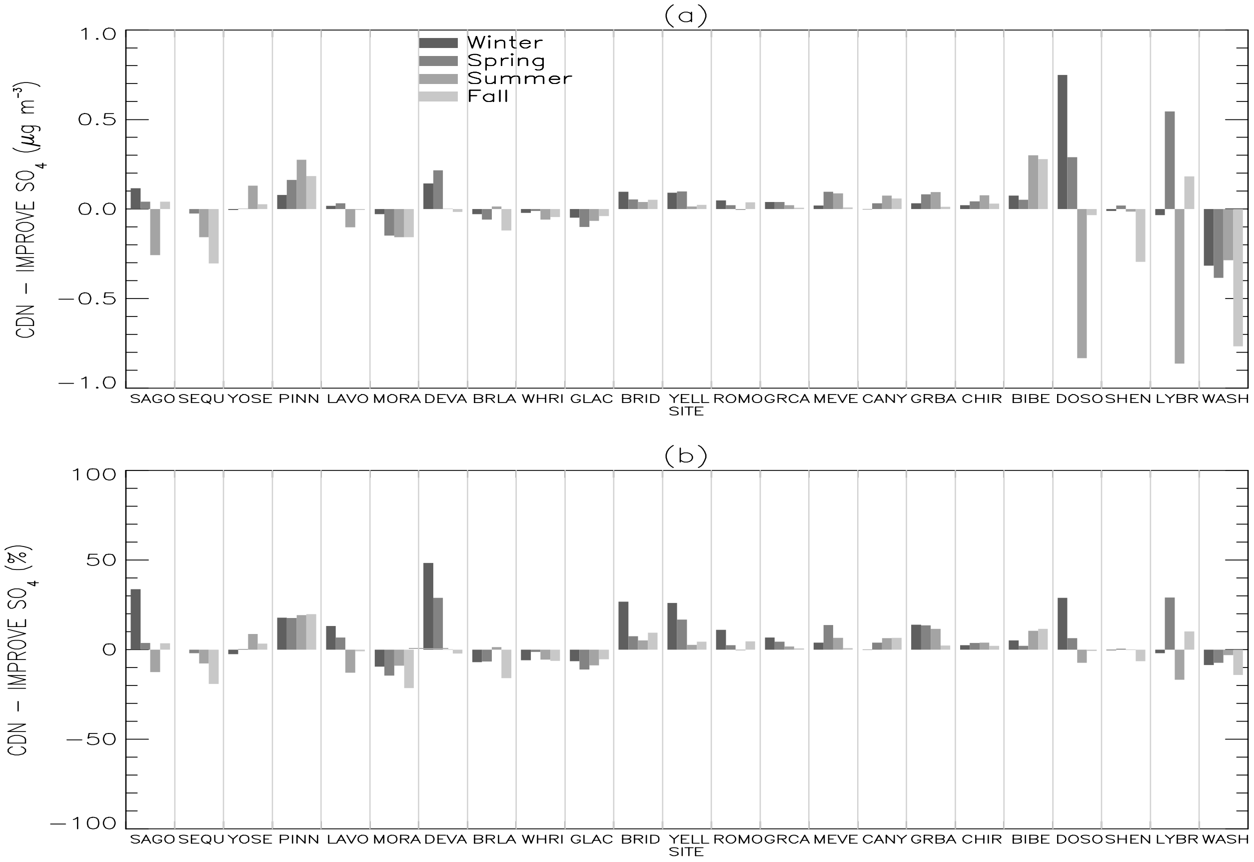

Figure G.7 *(a) Absolute difference in particle* SO_4^{2-} *mass by season. (b) Relative difference in particle* SO_4^{2-} *mass by season.*

G.4.3.2 Nitrate

Figures G.8a and G.8b show analogous plots to those in Figure G.7, but for the seasonal comparison of particle NO_3^-. Note the relative scale in Figure G.8b is from –100 to +300%. In Figure G.8a and G.8b, wintertime data at SEK-SEQU are not shown due to lack of sufficient comparison data. Most comparison sites shown in Figure G.8 have higher particle NO_3^- mass concentrations from the CDN than IMPROVE. Exceptions are found among most eastern sites and the JOT-SAGO and GLR-GLAC comparison sites. It is perhaps noteworthy that Glacier National Park and sites in the eastern United States are the only comparison sites among those considered that exhibit a strong wintertime maximum in ambient particle NO_3^- mass concentration. Among comparison sites in the western and interior desert/mountain regions the magnitude of particle NO_3^- mass concentration differences are generally lowest during the winter.

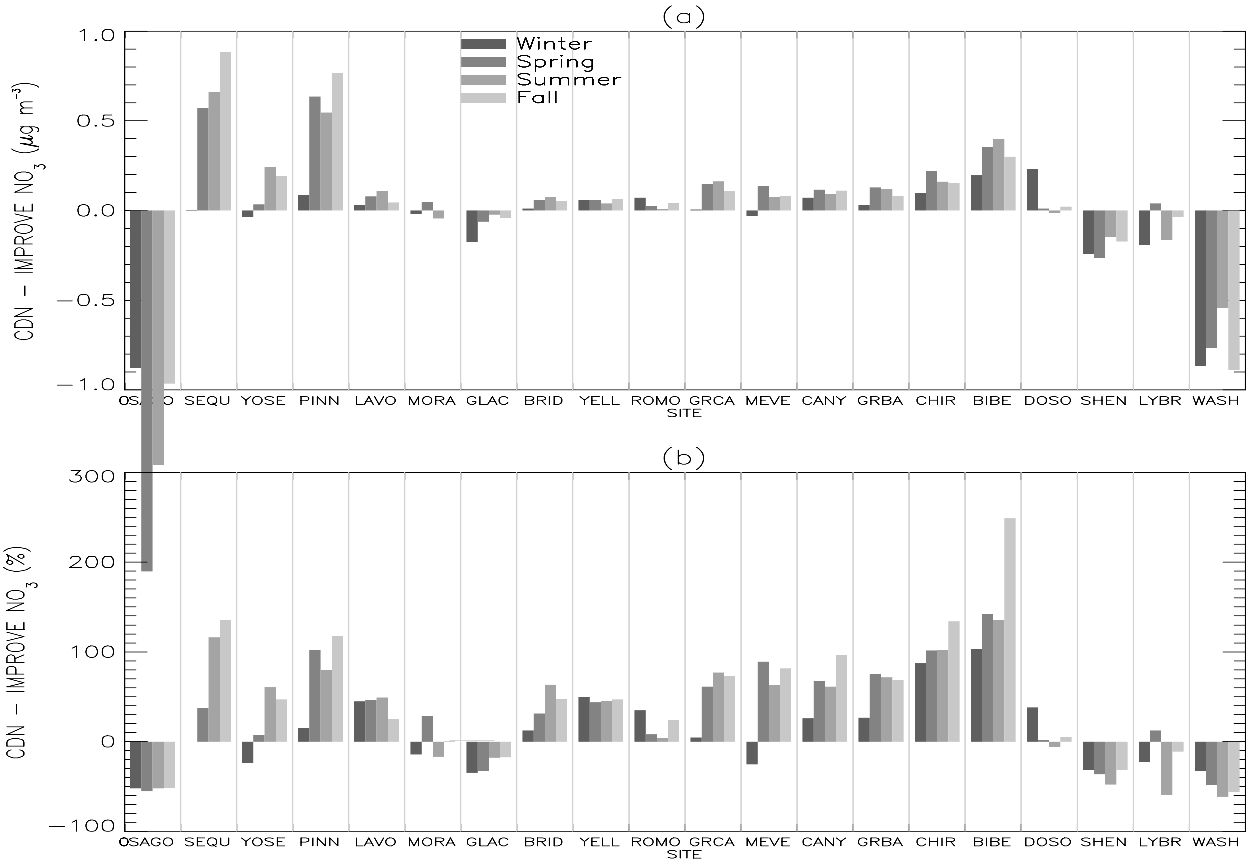

Figure G.8 *(a) Absolute difference in particle NO_3^- mass by season. (b) Relative difference in particle NO_3^- mass by season.*

G.4.4 Possible Explanations for Observed Particle NO_3^- Bias Related to Sampler Configuration

Because the observed relationship between ΔNO_3^-% and latitude elucidates no physical mechanisms that may explain ΔNO_3^-%, we look for relationships to other quantities having latitude dependence, which may also serve as indicators of mechanisms that cause the observed bias. Figure G.9 shows ΔNO_3^-% plotted against mean site temperature and the absolute particle NO_3^- mass concentration difference (ΔNO_3^-) expressed as a percent of coarse mass (CM) concentration for the 15 comparison sites shown in Figure G.6. The latitude dependence of temperature is intuitive, and CM concentrations are generally lower in the northern United States than in southern regions (Chapter 2.5.2). Figure G.9 indicates the mean site temperature increases proportionally to ΔNO_3^-%, suggesting a temperature dependent mechanism, such as the ammonium nitrate equilibrium, may play a role in the observed bias. Figure G.9 also shows the magnitude of ΔNO_3^- relative to CM increases as ΔNO_3^-% increases, suggesting particle NO_3^- associated with CM may explain some of the observed bias.

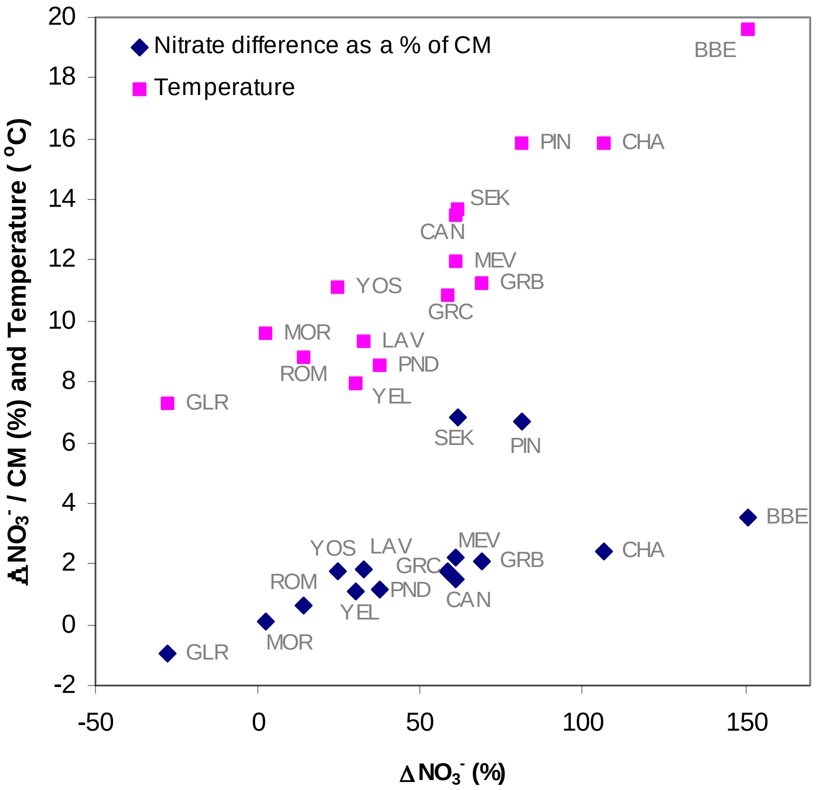

Figure G.9 *Two variables, $\Delta NO_3^-/CM$ and temperature, plotted against $\Delta NO_3^-(\%)$ for 15 comparison sites in the western and interior desert/mountain regions. CDN site acronyms are shown at each data point.*

Two outlying CM values in Figure G.9 are the PIN and SEK site pairs, which may be due to particle NO_3^- sampling characteristics at these sites indicative of urban, rather than rural, conditions. Linear correlation coefficients for ΔNO_3^-% to site latitude, temperature and CM (the latter excluding the PIN and SEK site pairs) are 0.9 or greater, and highly significant (P-values less than 0.001).

We use ordinary least-squares multiple regression to form a simple model of the observed particle NO_3^- bias is the interior desert/mountain region. We chose this region because it contains the greatest number of comparison sites, and particle NO_3^- data from some sites in this region display the largest magnitude relative bias among all comparison sites. In the regression, the absolute nitrate bias (ΔNO_3^-) is the dependent variable and temperature (T) and a CM tracer in the fine particle mode (CM_f) are independent variables. CM_f is defined as elements characteristic of soil and sea salt, where soil is the sum of common oxides of crustal elements (2.2*Al + 2.49*Si + 1.63*Ca + 2.42*Fe + 1.94*Ti) and sea salt is NaCl (2.5*Na) from IMPROVE Module A [Malm et al., 1994]. CM_f is used as a surrogate for CM because it is measured with more precision and accuracy than gravimetrically determined CM, and it has been shown to be the "tail" of the coarse particle distribution [Perry et al., 1997]. The multiple regression R^2, using means from the nine comparison sites in the interior desert/mountain region where $\Delta NO_3^- > 0$, is 0.96. Apportionment of ΔNO_3^- to CM_f and T in the regression is approximately 35:65, respectively. The results from the multiple regression are:

$$\Delta NO_3^- = -0.157 \quad + 0.013^{\pm 0.004}[T(^{o}C)] + 0.109^{\pm 0.043}[CM_f(\mu g\, m^{-3})] \qquad \text{(G.6)}$$

Equation (G.6) indicates that ΔNO_3^- increases as both mean site temperature and CM concentration increase for comparison sites in the interior desert/mountain region.

The positive correlation between ΔNO_3^- and temperature shown in Figure G.9 and indicated by Equation (G.6) is opposite to what would be expected if ammonium nitrate volatilization from Teflon in the CDN filter packs is responsible for the observed particle NO_3^- bias. However, this mechanism is consistent with higher particle NO_3^- mass concentrations from IMPROVE protocol measurements than from the CDN (as seen at GLR and some eastern comparison sites), if ammonium nitrate is volatilized from Teflon in the CDN filter packs. A study sponsored by the CDN found HNO_3 measured by its filter pack sampler is 11 to 12% higher than HNO_3 recovered from a collocated annular denuder sampler at a site in Indiana [CDN Deposition Summary Report, 1998]. Particle NO_3^- biases, with magnitudes up to 60% and attributed to ammonium nitrate volatilization from Teflon, have been observed during summer months [Chow et al., 1994; Hering and Cass, 1999].

The majority of comparison sites in the west and interior desert/mountain regions indicate particle NO_3^- mass concentrations measured using CDN sampling protocol are higher than those measured by IMPROVE protocol. If particle ammonium nitrate volatilization occurs in the IMPROVE denuder prior to collection on the Nylasorb substrate, then CDN particle NO_3^- could be higher than IMPROVE measurements (see Durham et al., [1986] for a discussion of HNO_3 release from particle NO_3^- in diffusion denuders). However, this mechanism is unlikely because the particle residence time in the IMPROVE denuder (about one second) is much less than the ammonium nitrate gas phase equilibration time scale which, although highly uncertain, is about 1 to 15 minutes [Wexler and Seinfeld, 1992]. Another mechanism that may explain a positive CDN bias is enhanced coarse particle NO_3^- collection efficiency for the non-size selective CDN sampler over that of the IMPROVE module fitted with a $PM_{2.5}$ cyclone. During the Subregional Cooperative Electric Utility, Department of Defense, National Park Service and Environmental Protection Agency (SCENES) Study [Benner et al., 1991], conducted in Arizona, filter packs operating without a cyclone (AeroVironment Filter Packs) measured higher particle NO_3^- mass concentrations than denuded samplers operating with cyclones under certain conditions. Zhang and McMurry [1992] suggest this bias may have resulted from collection of coarse particle nitrate by the filter pack samplers.

The magnitude of ΔNO_3^- relative to observed CM concentration is consistent with laboratory studies that indicate heterogeneous reactions between soil and/or sea salt particles and oxides of nitrogen and/or HNO_3 can form particle NO_3^- in amounts up to approximately 3% of coarse particle mass [Mamane and Gottlieb, 1992]. We do not interpret ΔNO_3^- as a direct measurement of coarse particle NO_3^- mass, although it is of interest to point out that while ΔNO_3^-% is in some cases large, the absolute particle NO_3^- bias expressed as a percent of CM is generally small. The positive correlation between ΔNO_3^- and temperature and CM shown in Figure G.9 and indicated by Equation (G.6) is consistent with a coarse particle NO_3^- mechanism explaining some of the observed bias.

G.5 SUMMARY

Particle SO_4^{2-} and NO_3^- mass concentrations reported by the CDN and IMPROVE network at nearby monitoring locations are compared with the intent to quantify biases that may be introduced from differences in the respective network's sampling protocols. Particle sampling following CDN protocol employs a filter pack with non-size selective inlet, while sampling under IMPROVE protocol employs separate modules fit with either $PM_{2.5}$ or PM_{10} inlets, as well as a denuded inlet on the particle NO_3^- module. The two networks also use different sampling frequencies, the CDN on a weekly schedule and IMPROVE on a 24-hour twice a week schedule.

An averaging time analysis was performed to estimate the magnitude of uncertainty in IMPROVE twice a week samples as a function of averaging time. Based on this analysis, we recommend using at least four weeks of IMPROVE particle SO_4^{2-} measurements to form a reliable estimate of the population mean. Variability in measured particle NO_3^-, relative to mass concentration observed at selected comparison sites used in this study, is greater than observed particle SO_4^{2-} variability and therefore we recommend that approximately 13 weeks of IMPROVE data be used to estimate a population mean for particle NO_3^-. At these recommended averaging times, the uncertainty in the respective species particle mass concentrations is about 10 to 20%.

The nonparametric Theil regression was used to discriminate additive from multiplicative bias between particle mass measurements from the two monitoring networks. In the Theil regressions, the CDN data are used as the independent variable. The regression slopes for the particle SO_4^{2-} comparison are generally close to one and intercepts close to zero. For the particle NO_3^- comparison, regression slopes are indistinguishable from one at six comparison sites and significantly less than one at 14 comparison sites. Among comparison sites in the west and interior desert/mountain regions the magnitude of particle NO_3^- regression slopes tend to decrease as the monitoring site latitude became more southerly, indicating CDN is multiplicatively biased higher than IMPROVE in these regions. All comparison sites have particle NO_3^- regression intercepts either significantly greater than, or indistinguishable from, zero.

Differences between mean particle SO_4^{2-} mass concentrations reported by the two monitoring networks are small (mean difference of 0% among all comparison sites, by geographic region). On the other hand, differences between mean particle NO_3- mass concentrations are substantial, with measurements from the CDN higher than those from IMPROVE among 14 of 16 sites in the west and interior desert/mountain regions. CDN particle NO_3^- mass concentrations are biased progressively higher than IMPROVE measurements as site latitude becomes more southerly, consistent with the north-south trend observed in the Theil regression slope magnitude. Among comparison sites in the east, mean particle NO_3^- mass concentrations from IMPROVE protocol measurements are generally higher than those from the CDN. Mean differences in particle nitrate are 40% in the west, 56% in the interior desert/mountain region, and –9% in the east, excluding locations with likely spatial variability between comparison sites.

Because the CDN filter pack sampler collects particles on a Teflon substrate, we anticipate loss of fine particle NO_3^- from the CDN samplers due to ammonium nitrate volatilization. In addition, we anticipate ammonium nitrate volatilization will not produce a significant sampling artifact in particle NO_3^- mass concentrations measured by the IMPROVE module operating with a denuded inlet and nylon collection substrate. Particle NO_3^- loss from the CDN filter packs may explain the observed bias at some comparison sites (e.g., some eastern United States sites) where particle NO_3^- mass concentrations measured using IMPROVE protocol are greater than those from the CDN. On the other hand, other mechanisms must be considered for cases where particle NO_3^- measured by the CDN is greater than that from IMPROVE. Coarse particle NO_3^- could produce a positive CDN bias if the cyclone on the IMPROVE NO_3^- module removes NO_3^- associated with coarse particles more efficiently than the non-size selective CDN inlet. However, our ability to accurately estimate the magnitude of the particle NO_3^- measurement bias related to one mechanism, such as coarse particle NO_3^-, may be confounded by the presence of an opposite bias related to a different mechanism, such as fine particle NO_3^- volatilization from Teflon in the CDN filter packs.

This study indicates particle SO_4^{2-} sampled using IMPROVE protocol can be used as a surrogate for similar measurement from the CDN, although particle NO_3^- measurements cannot. Bias between CDN and IMPROVE particle NO_3^- measurements is widespread and not easily explained due to the large number of sampling protocol differences between the two monitoring networks. Because most comparison sites used in this study are located in the western United States some conclusions reached herein may not be representative of areas with dissimilar ambient sampling conditions. This study points to a need for continued in depth and regionally specific comparisons of particle NO_3^- measurements from distinct sampler configurations either currently in use or intended for future air quality monitoring programs.

G.6 REFERENCES

Appel B. R., Tokiwa, Y., Haik M., and Kothny, E. L., Artifact particulate sulfate and nitrate formation on filter media, *Atmos. Environ.* 18(2):409-416, 1984.

Ashbaugh L. L., Eldred R. A., Hering S., Loss of particle nitrate from Teflon sampling filters: effects on measured gravimetric mass, California Air Resources Board, Final Report, Contract No. 96-305, September, 1998.

Benner C. L., Eatough D. J., Eatough N. L., and Bhardwaja P., Comparison of annular denuder and filter pack collection of HNO_3(g), HNO_2(g), SO_2(g), and particulate-phase nitrate, nitrite and sulfate in the south-west desert, *Atmos. Environ.* 25A(8):1537-1545, 1991.

Chow, J. C.; Fujita, E. M.; Watson, J. G. ; Lu, Z., Lawson, D. R., Ashbaugh, L. L., Evaluation of filter-based aerosol measurements during the 1987 Southern California Air Quality Study, Environmental Monitoring and Assessment, *Environ. Monit. Assess.*, 30(1):49-80, 1994.

Clean Air Status and Trends Network (CASTNet) Deposition Summary Report (1987-1995), EPA/600/R-98-207, July, 1998.

Durham J. L., Spiller L. L., and Ellestad T. G., Nitric acid-nitrate aerosol measurements by a diffusion denuder: a performance evaluation, *Atmos. Environ.*, 21(3):589-598, 1986.

Eldred, R. A., Cahill, T. A., Feeney, P., Comparison of independent measurements of sulfur and sulfate in the IMPROVE network, *Proceedings of the 86th Annual Meeting of the Air and Waste Management Association, paper # 93-RA-110.02*, Pittsburgh, PA, 1993.

Environmental Science and Engineering, Inc. (ESE), Comparison of CASTNet filter pack and annular denuder samplers – Interim data report (October 1996 – February 1997), Gainesville FL, 1997.

Graybill F. A. and Iyer, H. K., Regression Analysis: Concepts and Applications, Duxbury Press, Belmont California, 1994.

Harrison R. M. and Pio C. A., Size differentiated composition of inorganic atmospheric aerosols of both marine and polluted continental origin, *Atmos. Environ.* 17(9):1737-1738, 1983.

Hering S. V., Field comparisons of sampling methods for aerosol nitrate, In Aerosols: Formation and Reactivity, 2nd Int. Aerosol Conf. Berlin, Pergamon Journals Ltd., 1986.

Hering S. and Cass G., The magnitude of bias in the measurement of $PM_{2.5}$ arising form volatilization of particulate nitrate from Teflon filters, *J. Air and Waste Management Association*, 49(6):725-733, 1999.

Iyer H., Malm W., and Patterson P., Sampling duration calculations, Accepted for publication in *J. Air and Waste Management Association*, 2000.

Malm W. C., Sisler J. F., Huffman D., Eldred R. A., and Cahill T. C., Spatial and seasonal trends in particle concentration and optical extinction in the U.S. *J. Geophys. Res*. 99(D1):1347-1370, 1994.

Mamane, M. and Gottlieb J., Nitrate formation on sea-salt and mineral particles - a single particle approach, *Atmos. Environ.* 26A(9):1763-1769, 1992.

Mozurkewich, M., The dissociation constant of ammonium nitrate and its dependence on temperature, relative humidity and particle size, *Atmos. Environ.* 27A(2): 261-270, 1993.

Perry K. D., Cahill T. A., Eldred R. A., Dutcher D. D., and Gill T. E., Long-range transport of North African dust to the eastern United States, *J. Geophys. Res.* 102(D10):11,225-11,238, 1997.

Shaw R. W., Stevens R. K, Bowermaster J., Tesch J. W., and Tew E., Measurements of atmospheric nitrate and nitric acid: the denuder difference experiment, *Atmos.Environ.* 16(4):845-853, 1982.

Theil, H., A rank-invariant method of linear and polynomial regression analysis (I-III), *Proc. Kon. Ned. Akad. v. Wetensch. A.*, (53), 1950.

Turpin B.J., Saxena P., Allen G., Koutrakis P., McMurry P. and Hildemann L., Characterization of the southwestern desert aerosol, Meadview, AZ, *J. Air and Waste Management Association*, 47(3):344-356, 1997.

Wall S. M., John W., Ondo J. L., Measurement of aerosol size distributions for nitrate and major ionic species, *Atmos. Environ.* 22(8):1649-1656, 1988.

Wexler A. S. and Seinfeld J. H., Analysis of ammonium nitrate: departures from equilibrium during SCAQS, *Atmos. Environ.* 26A(4):579-591, 1992.

Wolff, G. T., On the nature of coarse continental aerosols, *Atmos. Environ.* 18(5):977-981, 1984.

Zhang X. and McMurry P. H., Evaporative losses of fine particulate nitrates during sampling, *Atmos. Environ.* 26A(18):3305-3312, 1992.